LAWRENCE
LIVERMORE
NATIONAL
LABORATORY

LLNL-JRNL-400630

Incorporation of probabilistic seismic phase labels into a Bayesian multiple-event seismic locator

S. Myers, G. Johannesson, W. Hanley

January 22, 2008

Geophysical Journal International

Disclaimer

Incorporation of probabilistic seismic phase labels into a Bayesian multiple-event seismic locator

Stephen C. Myers[1], Gardar Johannesson[2], and William Hanley[2]
[1]*Atmospheric, Earth, and Energy Department,*
[2] *Systems & Decision Sciences,*
Lawrence Livermore National Laboratory,
P.O. Box 808, L-205, Livermore, CA 94551
phone: (925) *423-4988, FAX:* (925) *423-4077, email: smyers*@llnl.gov

Date Received XXXX/XX/XX
Date Revised XXXX/XX/XX
Date Accepted XXXX/XX/XX

Abbreviated title: Probabilistic seismic phase labels

Corresponding Author: Stephen Myers
L-205
Box 808
7000 East Avenue
Lawrence Livermore National Laboratory
Livermore, CA 94551
USA

Abstract

We add probabilistic phase labels to the multiple-event joint probability function of Myers et al., 2007 that formerly included event locations, travel-time corrections, and arrival-time measurement precision. Prior information on any of the multiple-event parameters may be used. The phase-label model includes a null label that captures phases not belonging to the collection of phases under consideration. Using the Markov-Chain Monte Carlo method, samples are drawn from the multiple-event joint probability function to infer the posteriori distribution that is consistent with priors and the arrival-time data set. Using this approach phase-label error can be accessed and phase-label error is propagated to all other multiple-event parameters. We test the method using a ground-truth data set of nuclear explosions at the Nevada Test Site. We find that posteriori phase labels agree with the meticulously analyzed data set in more than 97% of instances and the results are robust even when the input phase-label information is discarded. Only when a large percentage of the arrival-time data are corrupted does prior phase label information improve resolution of multiple-event parameters. Simultaneous modeling of the entire multiple-event system results in accurate posteriori probability regions for each multiple-event parameter.

Introduction

Seismic analysis error is typically bundled into measurement precision or “pick” error (e.g. Billings et al. 1994). Numerous studies (e.g. Jefferies, 1932; Buland, 1976; Grand,

1990) find that travel-time residual distributions exhibit “heavy tails” with more outliers than expected by a Gaussian measurement error processes. Although it is convenient to bundle all analyst error into arrival-time measurement precision, this practice has resulted in a pervasive disagreement between analyst-assigned error and subsequent assessment of “pick” error, which may include more than arrival-time measurement error.

The over simplification of bundling analysis error into “pick” error is exemplified by the implicit acceptance of the analyst-assigned phase label (P, Pn, S, Sn etc.). A precise arrival-time or amplitude measurement may have large error if the phase is mislabeled or if a typographical error corrupts the analyst-assigned label. As such, correct phase identification is a critical component of seismic analysis that is often taken for granted, yet even an experienced analyst can be challenged to identify phases for a low-magnitude regional records. Data culling is the common tactic for dealing with phase label error. However, phase-label errors can be difficult to identify even using involved procedures. As a result, phase labeling error is a leading cause of erroneous data even after application of quality control procedures.

The differences between predicted travel times for the phases used in seismic analysis are typically far larger then the arrival-time measurement error. Therefore, arrival-time itself is a powerful indicator of phase name if location and travel-time prediction are sufficiently accurate. This fact can be exploited to identify phase names by simply comparing observed arrival times with the predicted arrival times for all phases under consideration. Recognizing the uncertainty in travel-time predictions, Engdahl et al.

(1998) reevaluated phase labels published in the International Seismic Center (ISC) bulletin by comparing observed arrival times to travel-time probability density functions for a number of phases. Using this approach, the probability of membership in a given phase distribution was calculated. Engdahl et al. (1998) then used the probability calculated for each potential phase name to randomly select a phase label. The reassigned phase labels were then used to relocate the ISC bulletin using a single-event locator. Engdahl et al. (1998) reported measurable improvement in event location, particularly depth estimates.

Several factors can confound the use of travel-time to aid in phase identification. Commonly, the same phase labels we wish to assess are the ones used to determine a preliminary event location. Because event location minimizes the difference between observed and prediction arrival-times, the location itself can absorb (be corrupted by) an error in the phase label, resulting in a phase label and arrival-time that are in agreement with predictions. Another confounding issue arises in instances where two phases arrive close in time, such as the cross-over in P-wave travel-times from local (crustal) Pg to regional (upper mantle) Pn. The Pn arrival can be small and lost in noise, resulting in the analyst mistaking Pg for Pn. Identification of depth phases for shallow events is also difficult because of the short time-delay relative to the first arrival (P). Although P should always arrive first, followed by pP and sP, the source radiation pattern can sufficiently diminish the amplitude of the P arrival creating confusion.

A number of useful phase identification methods have been developed that make use of 3-component records of ground motion (e.g. Jurkevics, 1988; Cichowicz, 1993; Tong and Kennett, 1995; Anant and Dowla, 1997) or a spatial array of seismograms (Ringdahl and Husebye, 1982; Kvaerna and Ringdal, 1992; Der et al., 1993). Ground particle motion can be indicative of wave type (P, S, Rayleigh, etc.), but phase identification (Pg, Pn, P, PKP) based on particle motion requires uncommonly clear signal. The velocity that a wave travels across an array of sensors (inverse phase slowness) can also be indicative of the phase name. Although bringing seismograms to bear on the phase identification problem is the best practice, use of these methods is not common throughout the seismic community for a variety of reasons. Readily available analysis software packages do not include sophisticated phase identification utilities and array stations are relatively few. As a result, the vast majority of phase labels found in bulletins are made at the discretion of the analyst.

In this study we incorporate phase identification into the Bayesian hierarchical multiple-event seismic location method (BAYHLoc, Myers et al., 2007). The BAYHLoc method formulates a joint posterior probability distribution over event hypocenters, travel-time corrections, and precision parameters for arrival-time measurements. Below we extend the joint probability of the multiple-event parameter space to include the phase name of each observation, and thus treat the phase label as a random variable. By incorporating assessment of phase label into a multiple-event locator we mitigate the confounding effects of event location error and travel-time prediction error. Further, instead of either accepting or rejecting a given phase label, the updated BAYHLoc method assigns phase

labels probabilistically. Therefore, phase-label uncertainty propagates to all other components of the multiple event parameter space. Further, the Bayesian methodology allows prior constraints on phase labels that may come from exceptionally clear signal or from waveform analysis.

Method

Notation

We follow the notation of Myers et al. (2007).

Event-origin *parameters* are:

x_i = (lat_i, lon_i, depth_i) = the *location* of the *i*-th event.

o_i = the *origin-time* of the *i*-th event.

The station data are:

s_j = (lat_j, lon_j, elevation_j) = the *location* of the *j*-th station.

a_{ijk} = the *k*-th measured *arrival-time* from the *i*-th event at the *j*-th station.

w_{ijk} = the *phase-label* assigned to the a_{ijk} arrival time, $w_{ijk} \in \Omega = \{1,2,\ldots, M\}$,

where M is the number of phase names under consideration and each integer corresponds to a seismic phase {Pg, Pn, P, Lg, etc.}.

The analyst-assigned phase-labels w_{ijk} are not necessarily correct. As such, we denote

W_{ijk} = the *true phase-name* (unknown) of the arrival a_{ijk}.

Phase label error may take two basic forms: 1) a phase in the set Ω that is mislabeled ($w_{ijk} \neq W_{ijk}$, $W_{ijk} \in \Omega$) and 2) a phase outside the set Ω that is mislabeled ($w_{ijk} \neq W_{ijk}$, $W_{ijk} \notin \Omega$). To account for phases not in the set Ω and erroneous arrival-time data, we introduce a

null phase-label, $W_{ijk} = 0$. While $w_{ijk} \in \Omega = \{1,2,\ldots, M\}$, we modify the true phase label such that $W_{ijk} \in \Omega^* = \{0,1,2,\ldots, M\}$.

Given a proposed event-location *x*, let

$F_w(x_i, s_j)$ = the *model-predicted travel-time* of phase *w* from event location *x* to station location *s*.

We further abbreviate the notation by letting $F_{ijw} = F_w(x_i, s_j)$. The model-predicted travel-time is only an approximation to the true (unknown) travel-time of each phase. We therefore explicitly define,

$T_w(x_i, s_j) = T_{ijw}$ = the *true travel-time* of phase *w* from event location x_i to station location s_j.

We will refer to a subset of parameters by simply dropping one or more subscripts. For example, a_{ij} denotes the collection of the n_{ij} arrival-times observed at station *j* from event *i*.

Hierarchical model

The framework closely follows Myers et al. (2007) in which the multiple-event location problem is decomposed into 3 components.

1) Travel-Time Model. The conditional distribution of the true travel-times (*T*) given travel-time predictions (*F*) and travel-time correction terms (τ);

$$p(T \mid F, \tau) \qquad (1)$$

2) Arrival-Time Model. The conditional distribution of the arrival-time data (a) given the origin times (o), the travel-times (T), phase configurations (W), and arrival-time error terms (σ);

$$p(a \mid o,T,W,\sigma) \tag{2}$$

3) Prior Model. A prior distribution for hypocenter parameters, arrival-time error terms, travel-time correction terms, and a prior distribution for phase configurations;

$$p(x,o), p(\sigma), p(\tau), p(W \mid w) \tag{3}$$

Using Bayes' theorem, these three physically related probability models are brought together in a joint posterior distribution

$$p(o,x,T,W,\sigma,\tau \mid a) = p(a \mid o,T,W,\sigma)\, p(T \mid F(x),\tau)\, p(W \mid w)\, p(x,o)\, p(\sigma)\, p(\tau) / p(a) \tag{4}$$

where $p(a)$ is the marginal distribution over the arrival-time data. Eqn 4 allows us to easily combine the 3 components of the hierarchical model to calculate the conditional probability for locations, travel-times, and phase-name configurations given a set of arrival-time data. The only difference between the above formulation and the formulation in Myers et al. (2007) is the prior model for phase labels. In Myers et al. (2007) the true phase configuration W was assumed equal to the input phase configuration w with probability 1. That is, $p(W = w \mid w) = 1$.

Myers et al. (2007) describe the travel-time correction (τ in Eqn 1) and arrival-time precision (σ in Eqn 2) models in detail. Summarizing, the travel-time model is specified as:

$$\delta_{ijW} = T_{ijW} - F_{ijW} = \alpha_W + \beta_W \left\| x_i - s_j \right\| + \gamma_{ijW} \quad (5)$$

where α_W and β_W are broad-area, phase-specific shift and scaling parameters, $\|x_i - s_j\|$ is the event-station distance, and γ_{ijW} is a path-specific correction term. The α term is a static shift in the travel-time curve of a given phase. The β term is a correction to the slope of the travel-time curve.

The arrival-time measurement model is specified in terms of the travel-time residuals

$$r_{ijW} = a_{ijW} - \left(F_{ijW} + \alpha_W + \beta_W \left\| x_i - s_j \right\| \right) \quad (6)$$

which are assumed *a priori* to have zero mean and inverse variance (i.e., precision) equal to ϕ_{ijW}. The residual precision is decomposed into event (ϕ_i), station (ϕ_j), and phase (ϕ_W) components, with $\phi_{ijW} = \phi_i \phi_j \phi_W$.

Phase-label prior model

As mentioned in the introduction, there is a diversity of methods by which a phase label may be determined. As such, there may be reason to give high probability (of being correct) to some input phase labels, whereas there may be only moderate probability that other phase labels are correct. The phase-label prior model formalizes how prior information on the phase label is used in BAYHLoc.

The phase label model starts with the full set (permutation) of possible phase labels for each event-station (W_{ij}). The phase label permutation is formed by considering that the correct phase name may be any of the labels established by the set Ω^*. Recalling that the set Ω^* includes the null phase label, the permutation includes the possibility that any or all of the phase labels do not belong to the set of seismic phases under consideration. For example, if three phases are under consideration {Pn, Pg, Lg} and 2 phases are input for a given event/station {Pn, Pg}, then W_{ij} has 13 possible configurations (Table 1), and we denote this phase configuration set by Θ^*_{ij}.

We note that it is possible to create phase label combinations that are not physical, or highly improbable. For instance, if Pn and Lg are the phases under consideration, then any case in which the phase labeled Lg arrives before Pn is not physical and should not be considered. Likewise, although Pg can arrive before Pn, it is highly unlikely that the head wave can be detected in the Pg coda. We, therefore, establish the set of permutations that can physically occur ($\widetilde{\Theta}^*_{ij}$), which is a subset of Θ^*_{ij}, and given by

$$\widetilde{\Theta}^*_{ij} = \{W_{ij} : W_{ij} \in \Theta^*_{ij},\ W_{ijk} < W_{ijl} \text{ for all } k < l \le n_{ij} \text{ where } W_{ijk} \text{ and } W_{ijl} \neq 0\ \}. \qquad (7)$$

Eqn 7 states that the elements of $\widetilde{\Theta}^*_{ij}$ are comprised of combinations of W_{ij} such that the arrival time order of the phase labels is established *a priori* with the order given by Ω_{ij}, with the phase labeled as 1 arriving before 2, 2 before 3, etc. The null phase label is exempt from arrival time order constraint.

The *a priori* probability of each element of W_{ij} are determined by two user-provided parameters: 1) the probability that the phase label is correct (π), and 2) the probability that the true phase label could be null (η). The prior probability that the true phase names are W_{ij} given that the input phase labels are w_{ij} is given by

$$p(W_{ij} \mid w_{ij}) = \begin{cases} \frac{1}{Z_{ij}} \prod_{k=1}^{n_{ij}} f_{ijk}(W_{ijk}, w_{ijk}) & \text{if } W_{ij} \in \tilde{\Theta}_{ij}^{*} \\ 0 & \text{otherwise} \end{cases} \tag{8}$$

where

$$f_{ijk}(W_{ijk}, w_{ijk}) = \begin{cases} \pi_{ijk}, & \text{if } W_{ijk} = w_{ijk} \\ \eta_{ijk}(1-\pi_{ijk}), & \text{if } W_{ijk} = 0 \\ (1-\eta_{ijk})(1-\pi_{ijk})/(M-1), & \text{if } W_{ijk} \neq w_{ijk}, W_{ijk} \neq 0, \text{and } M > 1 \end{cases} \tag{9}$$

In Eqn 8 Z_{ij} is a normalizing constant and M is the number of phases under consideration. We see from Eqn 8 that the probability of a given phase configuration W_{ij} is computed by multiplying the marginal probabilities of the individual members of the set W_{ij} and normalizing across all viable possibilities. Note that the probability is zero if the set W_{ij} violates the *a priori* arrival-time order.

The prior probability of each member of W_{ij} depends on whether the label under consideration equals the input phase label ($W_{ijk} = w_{ijk}$) and whether the label under consideration is null ($W_{ijk} = 0$). If the label under consideration equals the called phase label, then the probability is set to the user-provided prior probability (π_{ijk}). If the label under consideration is null, then the probability is the user-provided probability that the phase could be erroneous times one minus the *a priori* probability that the phase label is correct. For example, if η_{ijk} is 1 (not an advisable choice) then the only phase labels

considered are the input label and the null label. Setting η_{ijk} to 0.5, implies that if the input phase label is wrong, then the remaining probability is divided between the null phase and the set of all other remaining phase labels under consideration (minus the called phase label). Using Eqn 9 a value of η_{ijk} can be selected such that the remaining probability that the input phase is not correct (1- π_{ijk}) is evenly distributed over all other phase labels, including null. It is also straightforward to select both π_{ijk} and η_{ijk} such that the prior probability is evenly distributed across all phase labels, ignoring the provided phase label; below we refer to this case as a flat prior. Table 1 includes the probabilities of each phase combinations for an example where three phases are considered {Pn, Pg, Lg} and 2 phases are included for a given event/station {Pn, Pg}. In the example π_{ijk} = 0.9 and η_{ijk} = 0.5; Pn must arrive before Pg; and Pg must arrive before Lg. As expected, the highest probability phase combination is the one in which the input phase labels are correct, followed by the cases where one of the phase labels is erroneous, followed by the cases where both phases are erroneous, followed by all other possibilities in $\widetilde{\Theta}_{ij}^{*}$. Note that the joint probability that both phases are correct is greater than the product of the two marginal probabilities. This result occurs because the marginal probability of one phase label does not take into consideration the phase-order constraint of Eqn 7. After normalizing by the phase-order constraint the probability of a valid phase set is higher than expected.

Posteriori phase-label probability

We use the Markov-Chain Monte Carlo (MCMC) method to draw samples from the posteriori distribution. The samples are used to infer the joint probability across the multiple-event parameter space, including phase name probabilities.

Myers et al. (2007) present the BAYHLoc implementation of MCMC in detail, and we provide a brief summary here. The MCMC sampler generates a chain of parameter states (configurations) using stochastic transition kernels (samplers), where the next state of the chain is generated conditional on the current state. The behavior of the transition kernels is guided by the arrival data model, the travel-time model, and the priors (and in some cases by an additional next-state proposal distribution). In practice, parameter updates are conducted on one component of the hierarchical model at a time, while all other parameters are held fixed. In the BAYHLoc implementation, such component-based updates are carried out either by Metropolis random walks, Gibbs samplers, or slice samplers; see Myers et al. (2007) for details. Stepping through updates of each set of parameters completes one update of the entire parameter space. Gelman et al. (2004, section 11.5, pp 292) confirm that the progressive sampling is equivalent to simultaneous sampling from the joint probability function (Eqn 4). Typically, multiple Markov chains are generated (often in parallel), each consisting of thousands of posteriori samples, to infer the joint posteriori population.

Details of the stochastic transition kernels used to generate locations, travel-time corrections, and measurement precision parameters are provided in Myers et al. (2007). Here we focus on the sampler used to generate phase configurations.

A Gibbs sampler is used to generate a new phase configuration for each event-station pair. When all the parameters of the BAYHLoc model are held fixed except W_{ij}, the only part of the posterior probability distribution (Eqn 4) that changes with W_{ij} is given by

$$p(a_{ij} \mid A_{ij}, W_{ij}, \sigma)p(W_{ij} \mid w_{ij}) \tag{10}$$

where a_{ij} is the observed arrival time vector, A_{ij} is the predicted arrival time vector of all phases under consideration, and σ represents the arrival-time measurement model (Eqn 5). The first term represents the probability that the arrival-time data could occur given the predicted arrival times and the assumed phase labels and measurement error (and implicitly the hypocenter and travel-time model). The second term consists of the priors on the phase configuration, computed from Eqn 7. A Gibbs update of W_{ij} is accomplished by computing Eqn 10 for all possible configurations of W_{ij} (under consideration) and randomly selecting one configuration, with probability proportional to Eqn 10. Hence, W_{ij} configurations that do not fit the observed arrival-times and/or have low prior probability have a lower chance of being selected.

As outlined in Myers et al. (2007), the arrival-data distribution $p(a_{ij} \mid A_{ij}, W_{ij}, \sigma)$ of Eqn 10 is given by the product of n_{ij} Gaussian distributions, where the k-th Gaussian arrival distribution has mean given by A_{ijW} and inverse variance ϕ_{ijW}; $W = W_{ijk}$ and W_{ijk} is a valid phase (i.e., not null). What remains to be specified is the arrival distribution in the case where $W_{ijk} = 0$. Developing an error model for the outlier phase label is less straightforward.

Previous studies (e.g. Jeffreys, 1932; Buland, 1986) demonstrate that empirical travel-time residual distributions can be fit by a mixture of two Gaussian distributions; one Gaussian is used to fit the bulk of the residuals and the other Gaussian fits the "heavy tails" of the distribution (i.e. outliers). In the approach presented here we suggest that the heavy tails of the residual distribution are not members of the Gaussian arrival-time measurement error distribution but are instead phase-label errors (i.e. $w_{ijk} \neq W_{ijk}$). With this framework in mind we take the outlier arrival distribution to be Gaussian with mean given by A_{ijW}, where $W = w_{ijk}$ (the input label), and standard deviation d_0. It is reasonable to believe that the arrival-time distribution for the null-phase label is centered on the predicted time of the reported phase. We believe this to be reasonable because most reported phase labels are based on an iterative approach of picking phases and locating the event, making mistaken phase labels consistent with the proposed location. In the tests that follow we set d_0 to 600 seconds, but this number can be adjusted. In the case where the measurement error of a valid phase is 0.5 seconds, the null phase will be sampled with probability equal to the valid phase when the arrival-time residual is 1.885 seconds, or at 3.77 standard deviations from the mean. If measurement error doubles to 1.0 seconds then the valid and null phase are chosen with equal probability at 3.58 standard deviations from the mean, a small change. We find that within typical measurement errors, a static value for d_0 does not strongly affect the point in the valid-phase distribution at which a phase label is equally likely to be accepted as a valid or null phase. Therefore, we find that an adaptive approach for determining d_0 is not warranted.

Application

The examples below demonstrate 3 critical aspects of the BAYHLoc phase identification method. First, in the vast majority of instances phase names are identified with high probability. Second, the probability of all phase names is provided, which is useful in the few cases where a single phase name is not identified with overwhelming probability. Third, because BAYHLoc is a joint posteriori probability across all multiple-event parameters, the phase label uncertainty is propagated to the marginal probability of all other parameters including hypocenters.

Test data set

We test BAYHLoc phase identification with the Walter et al. (2004) data set of Nevada Test Site (NTS) explosions (Fig. 1). This data set is ideal for testing because the 74 event locations are known and the arrival data have been meticulously measured by an experienced analyst (Ryall, 2005). As part of the data set compilation, Walter et al. (2004) isolated timing errors by re-examining waveform data acquisition logs and evaluating the temporal evolution of travel-time residuals at each station. In cases where waveforms were not available, picks from the National Earthquake Information Center (NEIC) augment the arrival-time data set. Only NEIC phase arrivals within 3 standard deviations from the empirical curves are accepted.

Data set corruption

Table 2 summarizes the results for 29 test cases. Case categories are:

1) B = Walter et al. (2004) phase labels. These are the phase labels determined through careful analysis.

2) O = outlier. A percentage of the arrival data set was randomly selected and an arrival-time error was added. The arrival-time error was randomly drawn from a flat distribution with bounds of ±600 seconds. This case is meant to test the response to erroneous arrivals.

3) S = switched phase labels. A percentage of the arrival data set was randomly selected. The selected phase label was then switched with one of the other phase labels for that event and station. This case is meant to test the response to typographical errors and/or analyst mistakes.

4) M = mislabeled. This case is similar to "S", but instead of switching two phase labels one of the phases is removed from the data set. This case is more difficult to detect than "S", because removal of the second datum reduces the amount of information in the data set as a whole.

Prior assumptions

We tested the influence of prior information on the posteriori distribution by assuming one of three scenarios. In Table 2 the prior constraints are included in the case name following the colon:

1) AK = assumed known. The input phase labels are given a probability of 1.0.

2) IP = informative prior. The probability of a correct input phase label is set to 0.8 (π_{ijk} =0.8 in Eqn 9), and the probability that an incorrect phase is the erroneous is 0.5 (η_{ijk} =0.5 in Eqn 9). We find that these setting are appropriate for most data sets, giving consideration to the analyst

assessment while testing other possible phase labels against the expected arrival-time.

3) FP = flat prior. Both π_{ijk} and η_{ijk} are chosen such that all possible phase labels for each event/station are given equal probability. In other words, the input phase labels are ignored.

In the tests below we explicitly place prior constraints on the arrival order (see Eqn 7), with Pn assumed to arrive first, followed by Pg, and then Lg; see the example given in Table 2. In addition, locations and origin times for 3 of the events are constrained (assumed known), which effectively constrains the travel-time predictions for all events (Myers et al., 2007). Otherwise, the remaining prior parameters were specified to yield vague prior information.

Results, posteriori phase name probability

We compare the posteriori assessment of phase labels and locations with the Walter et al. (2004) data set. The locations of these explosion events are unimpeachable. While the arrival-time data set is very high quality, there is some degree of uncertainty. As such, there is a small degree of error in the assessment of phase labels. However, we believe the use of real data is preferable to a synthetic data set, because a real data set includes all error processes, including processes that we continue to learn about. For succinctness, we refer to the Walter et al. (2004) data set as the baseline.

Results are summarized in Table 2 and Figure 2. The number following the test case in Table 2 indicates the percentage data corrupted (e.g. O50= 50% of the arrival-times are corrupted). The 2nd column of Table 2 lists the percentage of highest posteriori

probability phase labels that agree with the baseline data set (also see Figure 2, right side). When the baseline date are input (Case "B"), 99.6% and 98.2% of the posteriori phase labels agree with the input depending upon whether informative or flat priors are used, respectively. In all cases (including flat prior case) where phase labels are switched ("S" cases) or mislabled ("M"), greater than 97.8% of posteriori phase labels agree with the baseline data. In cases where 10% of the arrival-times are corrupted ("O10" case), greater than 99% (informative prior) and 97% (flat prior) of phase labels agree with the baseline. Agreement with the baseline data is diminished as the percentage of corrupted arrival times increases; for the O50:IP,FP cases 84.6% and 83.7% of phase labels agree with the baseline, respectively.

Figure 2 shows the input phase labels and the most likely posteriori phase labels as a function of event-station distance for cases in which 30% of the data are corrupted. The known event hypocenters are used in Figure 2 plotting (as opposed to the BAYHLoc relocations) to isolate phase label and arrival-time-measurement errors. Plotting the results in the context of travel-time shows that the phase labels make physical sense; the empirical travel-time curves defined by data (posteriori phase labels) are consistent with curves established using known locations. We note, however, that even in the uncorrupted case a few of the measurements are most likely outliers. In the cases where phase labels are switched, the most likely result is indiscernible from the uncorrupted case. In other words, if the arrival-time information is preserved and only the phase label information is corrupted, then the phase labels are robustly determined, regardless of prior information.

The 3rd column of Table 2 lists the percentage of phase labels with posteriori probability greater than 0.9 (high probability) that agree with the baseline data set. In cases where phase labels are switched or mislabeled, a large majority of the posteriori phase labels are determined with high probability, and greater than 97% of arrivals agree with the benchmark. Only by corrupting arrival-time does agreement between the posteriori and benchmark phase labels drop to the expected agreement with the benchmark (90%). Results begin to match the expectation when a large percentage of the arrival-times are corrupted because arrival-time corruption is drawn from a flat ±600 second distribution and many realizations are needed to sample the edges of the pick-error distribution where ambiguity occurs.

The 4th column of Table 2 lists mean epicenter error between all realizations and the known location. Epicenter error is also plotted as a function of percentage data set corruption in Figure 3. The uncorrupted case (B) establishes an average error of approximately 1.7 km. Location error is, for the most part, unchanged when a flat prior is used. The cases where phase labels are switched (S) also result in approximately 1.7 km error, regardless of the percentage of data corruption. In the mislabeled cases (M), in which some data are removed, location error increases slightly to approximately 2 km as the level of corruption reaches 50% of the data set. The increase in location error is due to fewer arrival-time data. The largest difference in location performance is seen in cases where the travel-times are corrupted. When only 10% of the data are corrupted, location accuracy is consistent with the uncorrupted case (~1.8km). Location error ramps up to 7.5

km and 17 km when 50% of the data set is corrupted, depending upon whether the prior is informative or flat, respectively. We also include O10:AK and O30:AK, in which arrival time outliers are introduced and phase labels are assumed known with probability 1.0. If arrival-times are corrupted and no attempt is made to catch outliers, then location results degrade drastically.

Ambiguous phase labels effect on location probability regions

In the vast majority of test cases (Table 2) one phase configuration (W_{ij}) is identified as having far higher probability than any other configuration. However, there are instances in which more than one phase configuration has appreciable probability. While other algorithms would necessitate choosing one phase label configuration, the BAYHLoc joint probability function propagates phase-label uncertainty to all other aspects of the multiple-event problem.

We find that phase-label ambiguity is most clearly manifested as an expanded, sometimes multimodal, epicenter probability region. In Figure 4a we show an example event location where the Walter et al. (2004) phase labels are used with an informative prior. Posteriori phase labels are unambiguous for 8 of the 9 stations observing this event. The possibility of several phase label combinations at station MNV are listed in Figure 4a. For this event, phase-label uncertainty results in an expansion of the epicenter probability region (Figure 4a) to the northwest and a slightly non-symmetric (non-Gaussian) probability region. In Figure 4b, we see that the northeast expansion of the epicenter probability region is the result of sample locations for which the MNV phase

configuration is unchanged from the input. Location samples in which the Pn datum is erroneous (ignored) and the Pg label is switched to Pn comprise the highest epicenter probability density region.

Data set corruption diminishes phase label resolution and inflates location confidence regions. In Figure 4c we show an event location (same event as Figure 4a) in which 30% of the phase-labels are corrupted and 30% of the data are removed (see description of case M30:IP above). By chance, data at 3 of the 9 stations observing the Figure 4 event were corrupted (stations DAC, LAC, and THP). Posteriori phase label probabilities are unambiguous (and in agreement with Walter et al., 2004) at all stations except MNV and LAC. The phase label ambiguity results in a bimodal epicenter probability region (Figure 4c). Figure 4d shows locations determined with each of the 3 most probable phase configurations. The most likely phase configuration (all prior labels are correct) results in one mode of the epicenter probability region. Locations with the next two most likely phase configurations comprise the second mode of the epicenter probability region, which is the mode centered on the known location (Figure 4, lower panel).

Discussion

Our tests suggest that phase-labels can be robustly determined in a multiple-event location algorithm. In most of our test cases (Table 2; Figures 2 and 3), posteriori phase label probabilities change little when informative or flat priors are used. We may infer from this result that when placed in the multiple-event context, the analyst provided

phase labels carry little information, as the label is robustly inferred from the arrival-time data.

It is important to acknowledge the cases where prior phase label information does improve posteriori probability of phase label and other multiple-event parameters. In the cases where a large percentage of the arrival-time data are corrupted, prior constraint on the phase labels can help to tighten the posteriori distribution of all parameters. The cases in point are O50:IP and O50:FP, in which 50% of the arrival-times are corrupted. In the former case an informative prior is used and 81% of the posteriori phase labels are determined with probability > 0.9. However, when a flat prior is used, 61% of the posteriori phase labels are determined with probability > 0.9. The effect of prior phase labels in these cases is also observed in the epicenter error, where average error reduces from 17.5 km to 7.5 km when prior information is used. Corrupting 50% of the arrival-time data is an extreme test. When 10% of the arrival-times are corrupted 99% and 94% of the posteriori labels are determined with probability > 0.9 for informative and flat priors, respectively. These findings suggest that for a variable-quality data set, which is generally the case, prior information on the highest quality data can help tighten the posteriori distribution.

The special case where travel-times (as a function of distance) for two phases cross also deserves comment. If measurements for both phases are input, then phase ordering constraint (Eqn 7) eliminates ambiguity immediately before and after the cross over. Although ambiguity does occur at the point of the cross over, the ambiguity does not

present a practical difficulty because both arrivals are accurately predicted, and the effect on the other parameters of the multiple-event problem is small. Nonetheless, if only one of the phases comprising a cross-over is input, then a phase-label prior may provide an important constraint.

Conclusions

We incorporate probabilistic assessment of seismic phase labels (e.g. Pn, Pg, Sn, Lg) into the BAYHLoc multiple-event location routine of Myers et al. (2007). The BAYHLoc method simultaneously models all aspects of the multiple-event system, resulting in an assessment of the joint posteriori probability density function. Using a Bayesian formulation, prior constraints on any of the model parameters may be imposed.

The phase label model consists of all permutations of phases under consideration for each station/phase. The posteriori set of modeled phases includes a null phase label that captures data determined not to be members of the phase set under consideration. We model the null phase with a broad Gaussian distribution centered on the predicted arrival time of the input phase. Previous efforts (Jefferies, 1932; Buland, 1986) model arrival-time residuals as the mixture of two Gaussians. The first Gaussian is narrow and the other is broad. We interpret the narrow Gaussian distribution as the measurement error and the broad Gaussian as an error in phase label (the null phase).

Testing the updated BAYHLoc method with a high-quality data set, we find that phase labels are unambiguously determined even if input phase labels are discarded. Corruption

of a small percentage of arrival-times does not significantly affect the result, but phase label priors do improve the result when a large percentage of the arrival-times are corrupted.

The results suggest that, when placed in a multiple-event context, arrival times carry far more information than phase labels. In other words, given accurate arrival-times we can determine the phase labels unambiguously. Phase labels provide additional information only when the arrival-times are imprecise. Heretofore, location methods force the input of one phase label per arrival, leaving only the option to accept or reject each datum (arrival-time/phase-label). By simultaneously modeling phase labels, we can salvage the portion of the measurement (the arrival-time) that carries the information needed to constrain event locations and travel-times.

Acknowledgements

The authors have benefited from numerous conversations with Bill Rodi. This work performed under the auspices of the U.S. Department of Energy by Lawrence Livermore National Laboratory under Contract DE-AC52-07NA27344.

References

Anant, K.S., and F.U. Dowla, 1997. Wavelet transform methods for phase identification in three-component seismograms, *Bull. Seismol. Soc. Am,* **87**: 1598-1612.

Billings, S.D., M.S. Sambridge, and B.L.N. Kennett, 1994. Errors in hypocenter location: picking, model, and magnitude dependence, *Bull. Seismol. Soc. Am,* **84**: 1978-1990.

Buland, R., 1986. Uniform reduction error analysis, *Bull. Seismol. Soc. Am,* **66**: 173-187.

Cichowicz, A., 1993. An automatic S-phase picker, *Bull. Seismol. Soc. Am,* **83**: 180-189.

Der, Z.A., D.R. Baumgardt, and R.H. Shumway, 1993. The nature of particle motion in regional seismograms and its utilization for phase identification, *Geophys. Jour. Int.*, **115**, (3), 39-57.

Engdahl, E.R., R. van der Hilst, and R. Buland, 1998. Global teleseismic earthquake relocation with improved travel times and procedures for depth determination, *Bull. Seismol. Soc. Am,* **88**: 722-743.

Grand, S. P. (1990), A possible station bias in travel time measurements reported to ISC, Geophys. Res. Lett., 17(1), 17–20.

Gelman, A., J.B. Carlin, H.S. Stern, and D.B. Rubin, 2004. Bayesian Data Analysis 2nd ed.). Boca Raton, Florida: Hapman and Hall/CRC.

Jefferies, H. 1932. An alternative to the rejection of observations, *Proc. Royal Soc. Of London. Series A.*, 137, No. 831, 78-87.

Jurkevics, A., 1988. Polarization analysis of three-component array data, *Bull. Seismol. Soc. Am,* **78,** 1707-1724.

Kvaerna, T., and F. Ringdal, 1992. Integrated array and 3-component processing using a seimic microarray, *Bull. Seismol. Soc. Am,* **82**: 870-882.

Ringdal, F. and E.S. Husebye, 1982. Application of arrays in the detection, location and identification of seismic events, *Bull. Seismol. Soc. Am,* **72**: S201-S224.

Ryall, F., 2005. Analysis summary of an assembled Western U.S. dataset. *Lawrence Livermore National Laboratory technical report, UCRL-TR-210751*, 20pp.

Myers, S.C., G. Johannesson, and W. Hanley, 1997. A Bayesian hierarchical method for multiple-event seismic location, *Geophys. Jour. Int.*, **171**, (3), 1049-1063.

Tong, C., and B.L.N. Kennett, 1995. Towards the identification of later seismic phases, *Geophys. Jour. Int.*, **123**, 948-958.

Walter, W.R., K.D. Smith, J.L O'Boyle, T.F. Hauk, F. Ryall, S. Ruppert, S.C. Myers, R. Abbot and D.A. Dodge, 2004. An assembled western United States dataset for regional seismic analysis. *Lawrence Livermore National Laboratory technical report, UCRL-TR-206630,* 17pp.

Tables

Table 1: Example permutation of possible phase labels for a case where {0,Pn,Pg, Lg} are the phases under consideration (0 is a null phase for erroneous data) and two phases {Pn, Pg} are assigned by the analyst/system. The joint probability of each phase combination as computed using Eqn 8 is also shown (see text for details).

Phase Label	Permutation of possible phase labels												
	1	2	3	4	5	6	7	8	9	10	11	12	13

Pn	0	0	0	0	Pn	Pn	Pn	Pg	Pg	Pg	Lg	Lg	Lg
Pg	0	Pn	Pg	Lg	0	Pg	Lg	0	Pn	Lg	0	Pn	Pg
%probability	0.3	0.1	4.8	0.1	4.8	87.0	2.4	0.1	0.0	0.1	0.1	0.0	0.0

Table 2. Summary of epicenter and posteriori phase label accuracy. Each row is an average of 10 realizations of the specified type of data corruption (cases). See text for case definitions. Average epicenter error is the mean error of all realizations. Phase label accuracy (relative to the Walter et al. data set) is provided for the most likely posteriori label, and for cases in which the posteriori probability is greater than 0.9. The number in parenthesis is the number of arrivals in the data set meeting the criteria. In the "most probable" case, numbers less than 1589 reflect removal of data in the corruption procedure.

Case	% correct phase label, most probable	% correct phase label, probability >0.9	Average Epicenter Error (km)
B:AK	100.0 (1589)	100.0 (1589)	1.7
B:IP	99.6 (1589)	99.8 (1575)	1.7
B:FP	98.2 (1589)	99.5 (1498)	1.8
O10:IP	99.2 (1589)	99.4 (1570)	1.8
O20:IP	98.6 (1589)	99.0 (1568)	2.1
O30:IP	96.9 (1589)	98.2 (1534)	2.8
O40:IP	94.0 (1589)	96.5 (1498)	3.5
O50:IP	84.6 (1589)	91.6 (1293)	7.5
S10:IP	99.6 (1589)	99.8 (1570)	1.7
S20:IP	99.6 (1589)	99.7 (1561)	1.7
S30:IP	99.4 (1589)	99.7 (1544)	1.7
S40:IP	99.2 (1589)	99.7 (1535)	1.7
S50:IP	98.9 (1589)	99.7 (1517)	1.7

M10:IP	99.5 (1543)	99.8 (1517)	1.7
M20:IP	99.1 (1493)	99.7 (1458)	1.7
M30:IP	99.0 (1442)	99.4 (1407)	1.8
M40:IP	98.4 (1394)	99.3 (1348)	1.9
M50:IP	98.1 (1345)	99.0 (1294)	2.1
O10:FP	97.1 (1589)	98.7 (1493)	2.0
O30:FP	94.7 (1589)	97.9 (1388)	2.8
O50:FP	83.7 (1589)	94.3 (0981)	17.1
S10:FP	98.2 (1589)	99.3 (1497)	1.8
S30:FP	98.3 (1589)	99.5 (1497)	1.8
S50:FP	98.3 (1589)	99.3 (1501)	1.8
M10:FP	98.3 (1543)	99.5 (1456)	1.8
M30:FP	98.1 (1442)	99.6 (1344)	1.9
M50:FP	97.8 (1345)	99.4 (1250)	1.9
O10:AK	90.0 (1589)	90.0 (1589)	45.1
O30:AK	70.0 (1589)	70.0 (1589)	201.0

Figure Captions

Figure 1. Ground truth dataset of Walter et al. (2004). a) Known locations of 74 nuclear explosions at the Nevada Test Site. b) Regional stations used in location tests.

Figure 2. Input and posteriori travel-times and phase labels (left and right columns, respectively) are plotted as a function of event/station distance. All plots are reduced to Pn travel-time and the known event locations are used to compute distance. The "Case" designation in the left column indicates the test case (see text). Symbols are used to designate the phase label. Color in the left column calls attention to corrupted data. Color in the right column calls attention to disagreement between the input an most probable posteriori phase label, except when the posteriori label is "0" (i.e. erroneous) where grey is used.

Figure 3. Epicenter error vs. percentage data corruption. Epicenter error is plotted on a logarithmic axis. Various types of data corruption are indicated by differing symbols. A "+" through the symbol indicates that a flat prior was used (i.e. input phase labels were ignored). Otherwise, an informative prior was used. See text for details on test cases and informative prior.

Figure 4. The effect of phase-label uncertainty on epicenter probability regions. The known location is at the origin, and the "+" is plotted at the maximum probability density (mode, a.k.a. epicenter estimate). a) Probability region for one of the few events with

ambiguous posteriori phase labels (case B:IP). Red indicates high probability density grading through yellow to white where probability density is low. Contours show areas encompassing 50% and 95% of the probability. b) Epicenter samples coded by phase configurations at station MNV. Distinct phase configurations can comprise distinct portions of the probability region. c) Same as a) except corrupted data are used (case M30:IP). The probability region becomes distinctly multimodal. d) same as b) except for case M30:IP. The bimodal probability region is the result of distinct phase configurations at stations MNV and LAC.

Figures

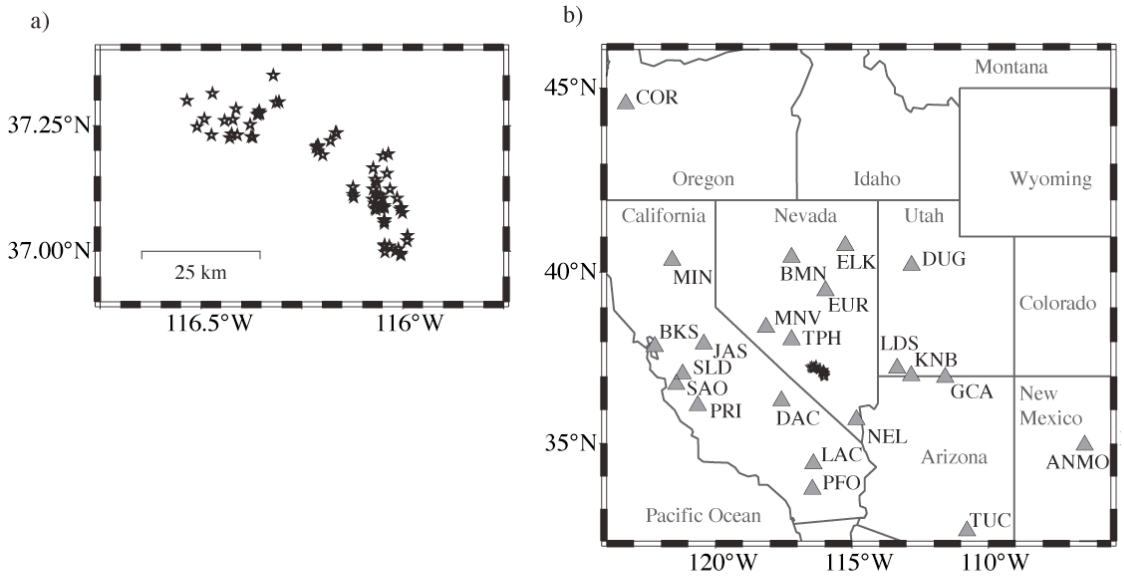

Fig. 1
Myers et al. 2008

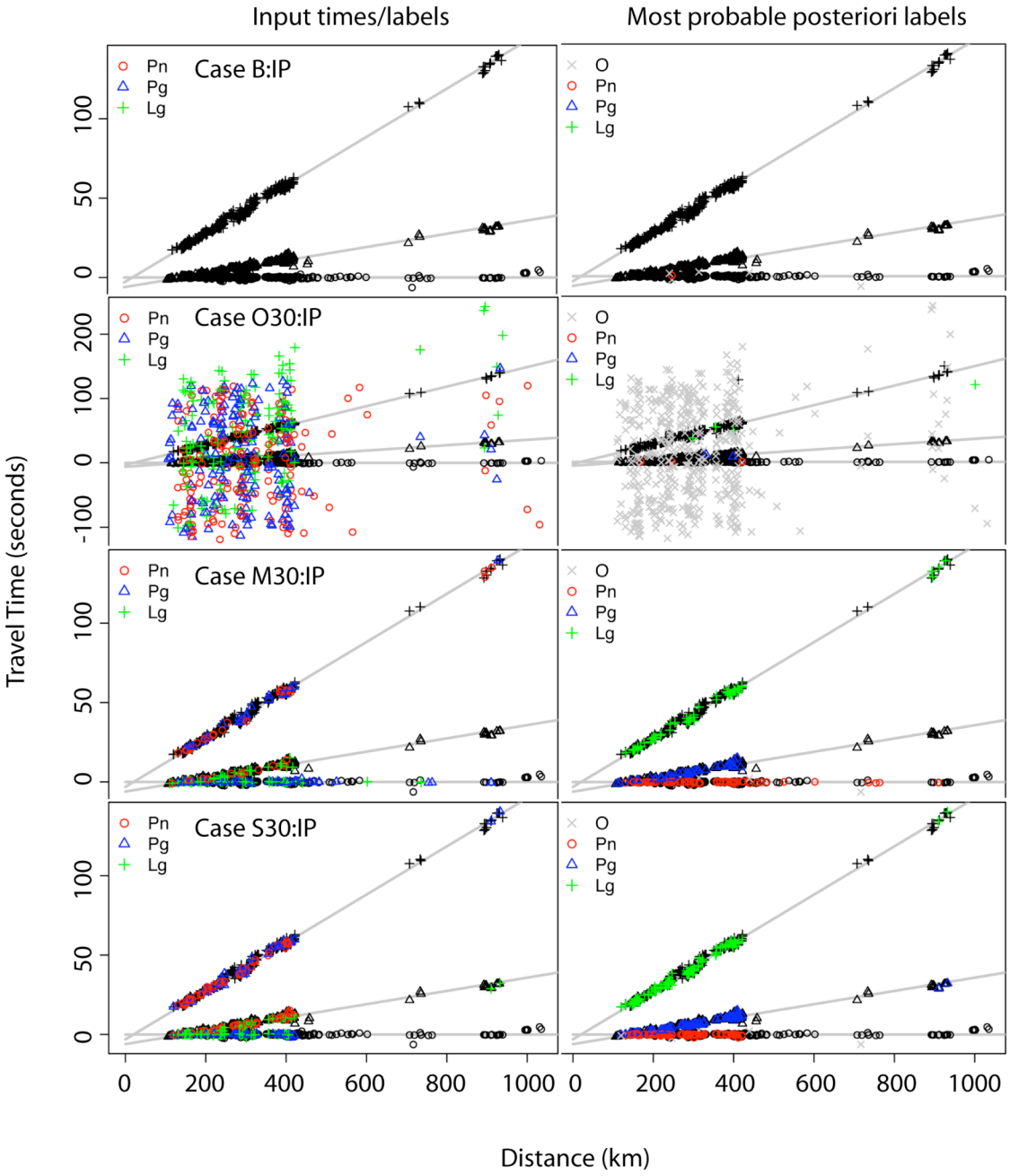

Figure 2
Myers et al., 2008

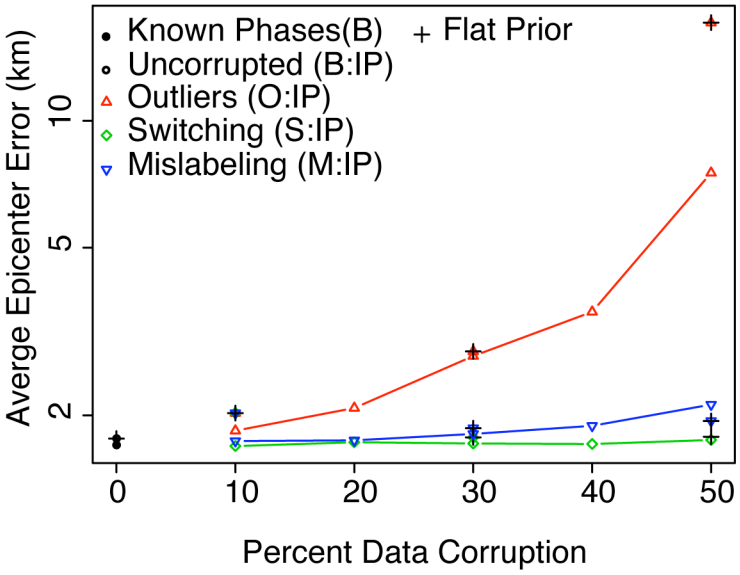

Figure 3.
Myers et al., 2008

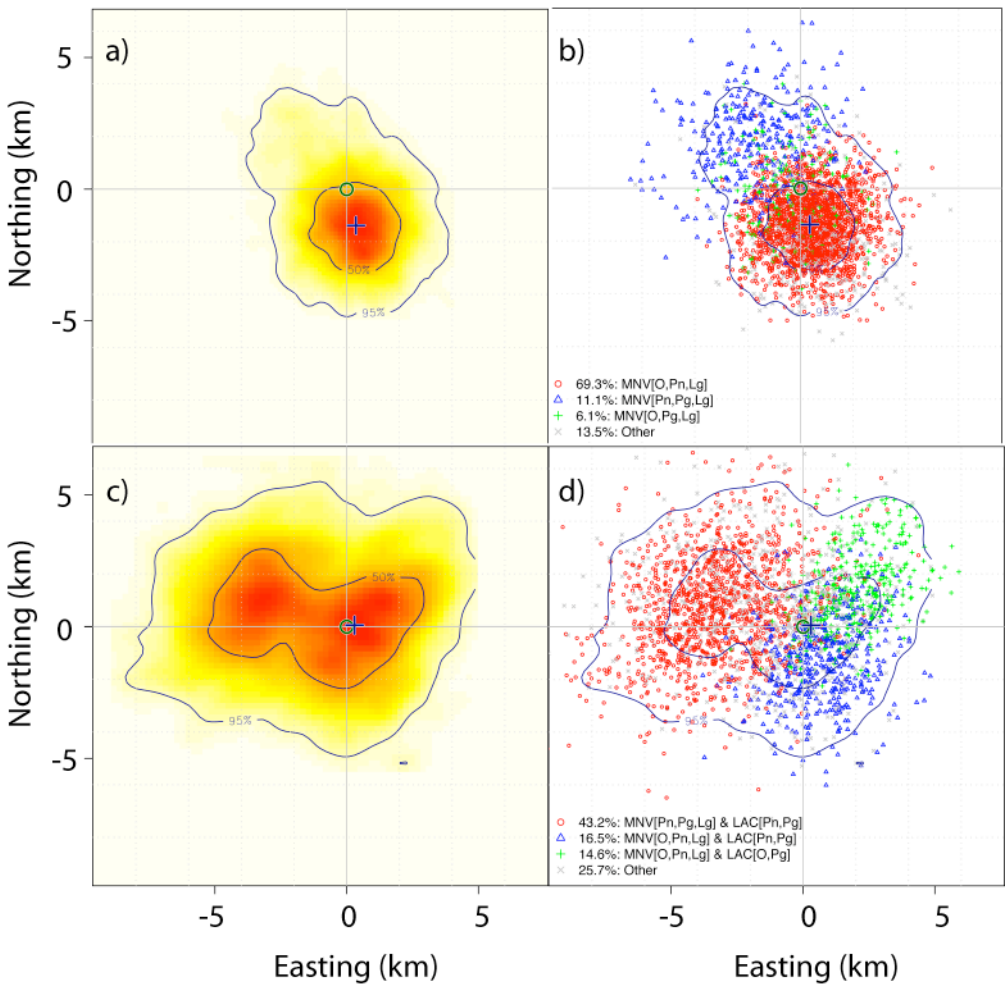

Figure 4.
Myers et al. 2008